Int. J. Heat Mass Transfer. Vol. 32, No. 9, pp. 1631–1639, 1989
Printed in Great Britain

0017-9310/89 $3.00+0.00

Theory of heat transfer-irreversible refrigeration plants

ADRIAN BEJAN
Department of Mechanical Engineering and Materials Science, Duke University, Durham, NC 27706, U.S.A.

(*Received* 6 *June* 1988 *and in final form* 10 *January* 1989)

Abstract—This study questions the view that the degree of thermodynamic imperfection (second law efficiency, η_{II}) of the refrigeration and liquefaction plants that have been built does not depend on the refrigeration load temperature T_L. It is shown first that when plotted correctly, the empirical η_{II} values decrease as T_L decreases. Two theoretical arguments are offered as explanations for this trend. The first argument is based on a refrigeration plant model the irreversibility of which is due solely to the 'internal' heat transfer that passes directly through the machine all the way to T_L. The second argument is based on a more refined model in which the refrigeration plant irreversibility is due to three heat transfer phenomena: the internal heat transfer (retained also in the first model), the external temperature difference between refrigeration plant and ambient, and the external temperature difference between the refrigeration load and the cold end of the refrigeration plant. It is shown that there exist optimum ways of allocating heat transfer equipment to the distinct parts of the plant, if the objective is to maximize the refrigeration capacity of the plant. Both theoretical arguments lead to the conclusion that η_{II} generally decreases as T_L decreases.

INTRODUCTION

THIS is the second part of a larger study of how heat transfer-type irreversibilities account for the aggregate inefficiencies of the large-scale power and refrigeration plants that have already been built. In the first part [1], it was shown that the recorded efficiencies of existing power plants can be anticipated on the basis of very simple models that include the irreversibility effect associated with the transfer of heat across a finite temperature difference. The objective of this second part is to show that the same methodology can be used in order to explain the observed trends in the inefficiencies of existing large-scale refrigeration plants.

The present work begins with taking another look at a well-known compilation of the performance characteristics of low temperature refrigerators and liquefiers [2–4]. This compilation is represented here by Fig. 1, which shows how the second law efficiency of these machines, η_{II}, decreases as the refrigeration or liquefaction capacity $\dot{Q}_L$ decreases, that is, as the machines become smaller. For future reference note that the second law efficiency of a refrigeration plant is defined as the coefficient of performance ratio

$$\eta_{II} = \frac{COP}{(COP)_C} \tag{1}$$

where $(COP)_C$ is the coefficient of performance of a Carnot refrigerator operating between the same temperature levels (T_H, T_L) as the actual machine the coefficient of performance of which is COP. The second law efficiency is recognized also as the rational or exergetic efficiency of the plant [5, 6].

The trend revealed by Fig. 1 is understood fairly well. The fact that the 'thermodynamic performance' of the refrigeration plant deteriorates steadily as the physical size of the plant decreases can be attributed to the greater role played by the heat loss to the ambient, as the machine shrinks in size. The least understood aspect of Fig. 1 is the question of whether η_{II} depends on the refrigeration load temperature T_L. About this figure Strobridge wrote in 1969 and, again, in 1974:

> "Historically the contention has been that higher temperature refrigerators (or liquifiers) are more efficient. The data for refrigeration temperatures between 10 K and 30 K (and 30 K to 90 K) refute that notion at least when presented on this common basis. To be sure, less input power is required to produce the same number of watts of cooling at higher temperatures, but the losses relative to ideal† are proportionally the same."

Strobridge's conclusion that

$$\eta_{II} \neq \text{function}\,(T_L) \tag{2}$$

is widely accepted. One very recent example is provided by Boyle and Riple's [7] study of refrigerator power requirements in space applications: the curves plotted on their Fig. 8 have been calculated by assuming that the second law efficiency is independent of the refrigeration load temperature T_L.

In this study, I argue that Strobridge's conclusion [equation (2)] is inappropriate, because if there is one

† The second law efficiency η_{II} in the present study.

NOMENCLATURE

C_e external conductance inventory, equation (14)
C_H external conductance allocated to the hot end, equation (12)
C_i internal conductance
C_i^* dimensionless internal conductance, equation (10)
C_L external conductance allocated to the cold end, equation (13)
C_t total conductance inventory, equation (25)
COP coefficient of performance, equations (6) and (17)
$(COP)_C$ coefficient of performance in the Carnot (reversible) limit, equation (7)
p_e price per unit of external conductance
p_r price per unit of internal resistance
P dimensionless group, equation (29)
$\dot{Q}_{HC}$ rate of heat rejection from the reversible part of the refrigeration plant
$\dot{Q}_i$ internal heat leak
$\dot{Q}_L$ refrigeration capacity (load)
Q^* dimensionless twice-maximized refrigeration load, equation (31)
$\dot{Q}_{LC}$ rate of heat transfer to the reversible part of the refrigeration plant
R_i internal thermal resistance, C_i^{-1}
T_H ambient temperature (all the T-type temperatures are thermodynamic temperatures)
T_{HC} high temperature seen by the reversible part (C) of the refrigeration plant
T_L refrigeration load temperature
T_{LC} low temperature seen by the reversible part (C) of the refrigeration plant
$\dot{W}$ mechanical or electrical power required by the refrigeration plant
x external conductance allocation fraction, equations (15)
y investment (C_t) allocation fraction, equations (26).

Greek symbols
η_{II} second law or rational efficiency, equation (1)
τ actual temperature ratio, T_H/T_L
τ_C temperature ratio spanned by the reversible part of the refrigeration plant, T_{HC}/T_{LC}.

Subscripts
C associated with the reversible (Carnot) part
max maximum
opt optimum.

effect that has been wiped out intentionally in drawing Fig. 1 it is the effect of the refrigeration temperature T_L (note the wide temperature ranges listed for the actual T_L values of the surveyed liquefiers and refrigerators). Whether T_L has any effect on η_{II} can only be determined by allowing T_L to vary while comparing machines of roughly the same size (capacity).

Lacking better data, I used the η_{II} values that I could read off Fig. 1 in the vertical column of width $10^2 \leqslant \dot{Q}_L \leqslant 10^5$ W, where $\dot{Q}_L$ is the refrigeration load.

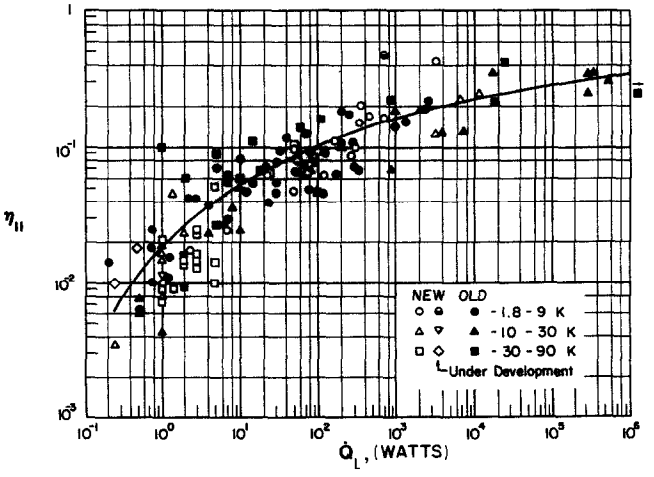

FIG. 1. The second law efficiency of constructed refrigeration and liquefaction plants [4].

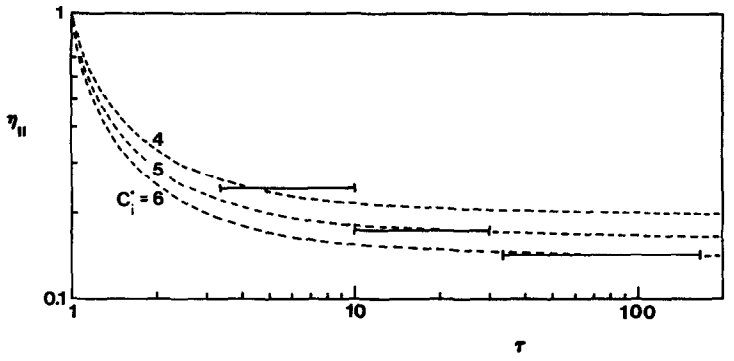

FIG. 2. Empirical data (horizontal bars) showing that η_{II} decreases as $\tau = T_H/T_L$ increases, and the theoretical curves based on the first model (dashed lines).

I sorted out these values according to the indicated temperature ranges (1.8–9 K, 10–30 K and 30–90 K) and obtained an average η_{II} value for each range. The three average values calculated in this manner are shown in Fig. 2: in each case the two extreme points of each horizontal bar indicate the width of the T_L range to which the calculated η_{II} value refers (note that T_H is the ambient temperature level, 300 K).

Figure 2 reveals a definite trend, this, despite the considerable degree of T_L averaging that was inherited from the way in which the data of Fig. 1 were sorted out originally. Higher temperature refrigerators have higher second law efficiencies indeed. The 'historical contention' criticized by Strobridge [3,4] appears to find support in the empirical information presented in Fig. 2.

The challenge now is to anticipate the general trends of Fig. 2 theoretically. In what follows I show that this fundamental thermal engineering question can be answered based on two very simple models of refrigeration plant operation.

THE FIRST MODEL

Consider the steady-state refrigeration plant model sketched in Fig. 3. According to this model the plant owes its irreversibility solely to the 'internal' heat transfer $\dot{Q}_i$ that flows through the machine 'vertically', i.e. from the ambient temperature level T_H to the cold-end temperature T_L. In an actual refrigeration plant $\dot{Q}_i$ represents the combined effect of vertical heat leaks through components such as:

(i) the counterflow heat exchanger alluded to in the fourth paragraph of the preceding section;

(ii) the supports that tie the cold end (T_L) mechanically to the room temperature frame of the machine;

(iii) the thermal insulation system sandwiched between T_L and T_H.

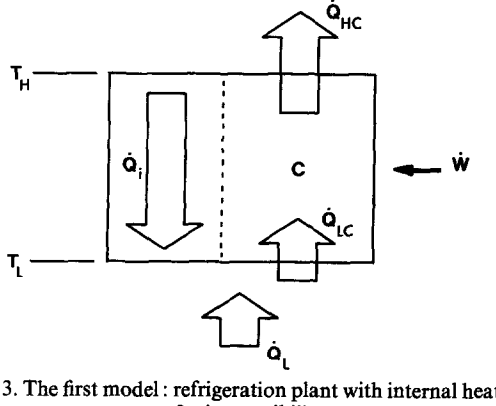

FIG. 3. The first model: refrigeration plant with internal heat transfer irreversibility.

In a machine of fixed size, the simplest model for the combined internal heat leak effect $\dot{Q}_i$ amounts to writing

$$\dot{Q}_i = C_i(T_H - T_L) \tag{3}$$

where the constant C_i is the internal conductance of the refrigeration plant. One could, of course, refine equation (3) by raising the temperature difference $(T_H - T_L)$ to a certain exponent, if radiation heat leaks and temperature dependent conductivities are dominant in the evaluation of $\dot{Q}_i$. It turns out that the simple linear model (3) captures enough of the heat transfer reality of the refrigeration plant in order to explain the downward trend revealed by Fig. 2.

The model of Fig. 3 consists of Carnot refrigerator working in parallel with the internal conductance discussed above. Applied only to the Carnot refrigerator, the second law of thermodynamics states that

$$\frac{\dot{Q}_{HC}}{T_H} = \frac{\dot{Q}_{LC}}{T_L} \tag{4}$$

in which $\dot{Q}_{LC}$ is to be distinguished from the refrigeration capacity (load) $\dot{Q}_L$, which is fixed

$$\dot{Q}_{LC} = \dot{Q}_L + \dot{Q}_i. \tag{5}$$

Using the second law (4) and noting also that the refrigerator power input $\dot{W}$ is equal to $(\dot{Q}_{HC} - \dot{Q}_{LC})$, the coefficient of performance of the overall plant is simply

$$COP = \frac{\dot{Q}_L}{\dot{W}} = \frac{1-\dot{Q}_i/\dot{Q}_{LC}}{T_H/T_L - 1}. \quad (6)$$

The Carnot limit of this coefficient is

$$(COP)_C = \left(\frac{T_H}{T_L} - 1\right)^{-1} \quad (7)$$

therefore, the second law efficiency of the actual plant modeled in Fig. 3 is

$$\eta_{II} = 1 - \frac{\dot{Q}_i}{\dot{Q}_{LC}} \quad (8)$$

or, after invoking equations (3) and (5)

$$\eta_{II} = \left[1 + C_i^*\left(1 - \frac{T_L}{T_H}\right)\right]^{-1}. \quad (9)$$

In this final result C_i^* is a dimensionless version of the internal conductance introduced first in equation (3), namely

$$C_i^* = C_i \frac{T_H}{\dot{Q}_L}. \quad (10)$$

It is already evident from the analytical form of equation (9) that η_{II} decreases monotonically as the refrigeration temperature level T_L decreases. The same point is made graphically in Fig. 2, which shows that a constant-C_i^* curve (the internal heat transfer constant C_i^* of which is of the order of 5) passes right through the band of η_{II} values calculated based on the data of Fig. 1. The second law efficiency decreases monotonically also as C_i^* increases (this trend should be expected, because refrigerated enclosures with larger heat losses make less efficient refrigeration plants).

One interesting observation made possible by Fig. 2 is that

$$C_i^* = \text{constant of the order of 5} \quad (11)$$

recommends itself as an empirical scaling law of the large population of built refrigeration plants compiled by Strobridge and Chelton [2]. This law states that the built-in conductance C_i scales with the refrigeration capacity $\dot{Q}_L$ and that the combined internal leak $\dot{Q}_i$ is consistently of the order of five times the refrigeration load $\dot{Q}_L$.

THE SECOND MODEL

To refine the model of the irreversible refrigeration plant means to account for more than the single source of irreversibility considered in the model of Fig. 3. Three irreversibility sources are recognized by the new model sketched in Fig. 4. These are the internal heat leak $\dot{Q}_i$ and the finite temperature differences $(T_{HC} - T_H)$ and $(T_L - T_{LC})$ required by the heat rejection and absorption rates associated with the remainder (reversible) part of the refrigeration plant.

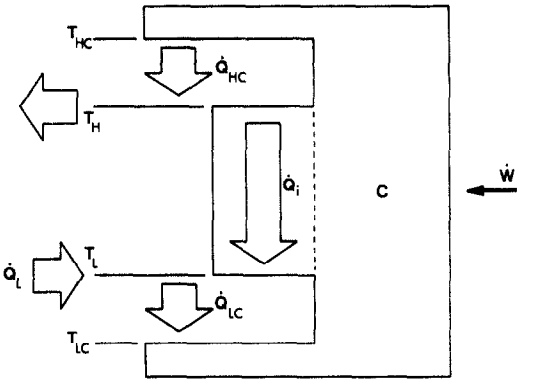

FIG. 4. The second model: refrigeration plant with internal and external heat transfer irreversibility.

Retaining the linear relation adopted already for the internal heat transfer rate, equation (3), we write that $\dot{Q}_{HC}$ and $\dot{Q}_{LC}$ are proportional to the respective temperature differences (see Fig. 4)

$$\dot{Q}_{HC} = C_H(T_{HC} - T_H) \quad (12)$$

$$\dot{Q}_{LC} = C_L(T_L - T_{LC}). \quad (13)$$

The proportionality factors C_H and C_L are the 'external' heat transfer conductances provided by the hot end and cold end heat exchangers, respectively. In heat transfer engineering terms, for example, the hot end conductance C_H scales as the product between the overall heat transfer coefficient and the total area of the hot end heat exchanger(s) (e.g. the battery of 'aftercoolers' or 'intercoolers' positioned between the stages of the compressor of a liquid nitrogen or liquid helium refrigerator). The end conductances are expensive commodities, because they both increase with the size of the respective heat exchangers. For this reason it makes sense to introduce as a design constraint the total external conductance inventory C_e [1]

$$C_e = C_H + C_L \quad (14)$$

and the conductance fraction x defined by the relations

$$C_H = (1-x)C_e \quad \text{and} \quad C_L = xC_e. \quad (15)$$

The analytical description of the model of Fig. 4 consists of equations (3), (12)–(15) and the second law statement for the reversibly operating part of the model

$$\frac{\dot{Q}_{HC}}{T_{HC}} = \frac{\dot{Q}_{LC}}{T_{LC}}. \quad (16)$$

We are interested in how the putting together of all the pieces of this model influences the overall par-

ameter η_{II}. To calculate the second law efficiency we note first that

$$COP = \frac{\dot{Q}_L}{\dot{W}} = \frac{1-\dot{Q}_i/\dot{Q}_{LC}}{\tau_C - 1} \tag{17}$$

where τ_C is shorthand for the absolute temperature ratio across the reversible part of the refrigeration plant

$$\tau_C = \frac{T_{HC}}{T_{LC}}. \tag{18}$$

Noting further that equations (5) and (7) apply also to the present model, it is not difficult to show that the second law efficiency is also equal to

$$\eta_{II} = \frac{\tau - 1}{\tau_C - 1}\left(1 + \frac{\dot{Q}_i}{\dot{Q}_L}\right)^{-1}. \tag{19}$$

In this expression τ is the actual temperature ratio seen from the outside of the refrigeration plant

$$\tau = \frac{T_H}{T_L}. \tag{20}$$

An essential part of the argument constructed here is the thought that the designer of the refrigeration plant is concerned first and foremost with the maximization of the service (benefit) furnished by the plant, not with 'efficiency'. This thought translates into maximizing whenever possible the refrigeration capacity $\dot{Q}_L$ per unit of capital invested in the machine. It is important to note also that this design philosophy is conceptually on the same footing as the treatment of irreversible power plants [1], according to which the designer's objective is to maximize the production of mechanical power per capital invested, not the energy conversion efficiency.

For the reason outlined above, we focus on the analytical composition of the $\dot{Q}_L$ function and, after using equations (12)–(16), find that

$$\dot{Q}_L = C_e T_H \left(\frac{1}{\tau} - \frac{1}{\tau_C}\right)(1-x)x - \dot{Q}_i. \tag{21}$$

The refrigeration load is maximized with respect to x if

$$x_{opt} = \tfrac{1}{2} \tag{22}$$

that is, if the external conductance inventory is divided evenly between the two ends of the machine. In what follows we assume that equation (22) always holds, in other words, that the $\dot{Q}_L$ formula (21) takes the simpler form

$$\dot{Q}_{L,max} = \frac{1}{4} C_e T_H \left(\frac{1}{\tau} - \frac{1}{\tau_C}\right) - \dot{Q}_i. \tag{23}$$

Combined with equations (3) and (23), the second law efficiency (19) emerges as a function of three variables (degrees of freedom), the external conductance inventory C_e, the internal conductance C_i and the 'Carnot' temperature ratio τ_C. It is possible to read directly off these equations the fact that η_{II} increases monotonically if C_e increases and if C_i decreases. The trend in C_i is similar to what we saw already in Fig. 2. The relationship between η_{II} and τ_C is not visible at this stage, therefore, we shall investigate it numerically.

Before plunging into numerical analysis, however, it is worth questioning whether C_e and C_i are truly independent. The concept of total external conductance inventory (C_e) was introduced as an economic constraint for the purpose of properly 'balancing' the sizes of the end heat exchangers. If C_e is recognized as something that is in short supply, then the internal resistance $R_i = C_i^{-1}$ is an expensive commodity also. That R_i is dear and comparable with C_e is illustrated by the main counterflow heat exchanger example (i) listed at the start of the preceding section. As a thermal insulation element oriented in the $(T_H) \rightarrow (T_L)$ direction, this heat exchanger is effective (i.e. its R_i is large) when its heat transfer area viewed in the stream-to-stream direction is large [8]. The internal resistance R_i of the counterflow heat exchanger is proportional to its total stream-to-stream heat transfer area, the latter being directly comparable (actually, competing in the budget) with the heat exchanger area represented by C_e.

The other internal heat leak path examples given in the preceding section can be analyzed similarly in order to reach the general conclusion that, like C_e, the internal resistance R_i is expensive. Although both C_e and R_i vary with the design, they are related through an economic constraint of the type

$$p_c C_e + p_r R_i = \text{constant} \tag{24}$$

where p_c and p_r are the prices of each additional unit of C_e and R_i. Dividing through p_c, we can rewrite equation (24) as

$$C_e + \frac{p_r}{p_c} R_i = C_t, \text{constant} \tag{25}$$

where C_t is the total external conductance that could be constructed with all the means available for constructing C_e and R_i, that is, with the right-hand side of equation (24). In any particular design C_e uses up only a fraction of C_t, therefore, calling this fraction y, we set

$$C_e = yC_t \quad \text{and} \quad \frac{p_r}{p_c} R_i = (1-y)C_t. \tag{26}$$

The net effect of the preceding two paragraphs is the conversion of the three-variable function $\eta_{II}(C_e, C_i, \tau_C)$ into a new relationship in which η_{II} depends on the investment fraction y, the price ratio p_r/p_c and the Carnot temperature ratio τ_C. This new formulation is preferable for two reasons, the first being the existence of an optimum y that maximizes η_{II}. This optimum thermodynamic balance between investing in external conductance inventory (C_e) and internal resistance (R_i) is qualitatively similar to the

optimum balance discovered between the hot end and cold end conductances, equation (22). Indeed, the refrigeration capacity maximized once already in equation (23) assumes the new form

$$\dot{Q}_{\mathrm{L,max}} = \frac{y}{4} C_{\mathrm{t}} T_{\mathrm{H}} \left(\frac{1}{\tau} - \frac{1}{\tau_{\mathrm{C}}} \right) - \frac{(p_{\mathrm{r}}/p_{\mathrm{c}}) T_{\mathrm{H}}}{(1-y) C_{\mathrm{t}}} \left(1 - \frac{1}{\tau} \right). \quad (27)$$

This expression can be maximized once more by choosing the optimum capital distribution ratio

$$y_{\mathrm{opt}} = 1 - 2P \left[\frac{\tau_{\mathrm{C}}(\tau - 1)}{\tau_{\mathrm{C}} - \tau} \right]^{1/2} \quad (28)$$

in which P is the dimensionless square root of the price ratio, defined by

$$p = \frac{(p_{\mathrm{r}}/p_{\mathrm{c}})^{1/2}}{C_{\mathrm{t}}}. \quad (29)$$

Substituting $y = y_{\mathrm{opt}}$ in equation (27) yields the twice-maximized refrigeration rate $\dot{Q}_{\mathrm{L,max,max}}$, which can be nondimensionalized as follows:

$$\frac{\dot{Q}_{\mathrm{L,max,max}}}{C_{\mathrm{t}} T_{\mathrm{H}}} = \frac{\tau_{\mathrm{c}} - \tau}{4\tau\tau_{\mathrm{C}}} \left\{ 1 - 4P \left[\frac{\tau_{\mathrm{C}}(\tau - 1)}{\tau_{\mathrm{c}} - \tau} \right]^{1/2} \right\}. \quad (30)$$

In the numerical work described next, the left-hand side of equation (30) is represented by the dimensionless number Q^*

$$Q^* = \frac{\dot{Q}_{\mathrm{L,max,max}}}{C_{\mathrm{t}} T_{\mathrm{H}}}. \quad (31)$$

The second reason for preferring the $\eta_{\mathrm{II}}(y, p_{\mathrm{r}}/p_{\mathrm{c}}, \tau_{\mathrm{C}})$ formulation is that in any given technological age the price ratio $p_{\mathrm{r}}/p_{\mathrm{c}}$ (or P) is likely to be constant. As the relative cost of building internal resistance and external conductance into each machine, the price ratio promises to change significantly (namely, to decrease) only upon the discovery of revolutionary ways of providing for the internal thermal resistance effect. Two examples of how inventions drove the $p_{\mathrm{r}}/p_{\mathrm{c}}$ ratio down over the history of low temperature refrigeration are the use of intermediate temperature expanders for cooling the main counterflow heat exchanger [9] and the use of advanced super-insulation techniques such as gas-cooled stacks of radiation shields [10, 11]. We shall return to this observation in the discussion of Fig. 8.

What is left now is to study the second law efficiency levels that can be attained if $\dot{Q}_{\mathrm{L}}$ is maximized twice, as indicated in equation (30). Substituting $y = y_{\mathrm{opt}}$ into the $\eta_{\mathrm{II}}(y, P, \tau_{\mathrm{C}})$ relation makes η_{II} a function of only P and τ_{C}. This function can be deduced easily from equation (19)

$$\eta_{\mathrm{II}}(P, \tau_{\mathrm{C}}) = \frac{\tau - 1}{\tau_{\mathrm{C}} - 1} \left[1 + \frac{P^2(\tau - 1)}{Q^* \tau (1 - y_{\mathrm{opt}})} \right]^{-1} \quad (32)$$

in combination with equation (28) for y_{opt} and equation (30) for Q^*. In this discussion we are assuming that the actual temperature ratio τ is a known constant.

Figure 5 shows that when the price ratio number P is fixed the second law efficiency reaches a maximum ($\eta_{\mathrm{II,max}}$) at a certain value of the Carnot temperature ratio, $\tau_{\mathrm{C,opt}}$. These optimum τ_{C} values are summarized as $\tau_{\mathrm{C,opt}}/\tau$ vs τ in Fig. 6. The discrepancy between $\tau_{\mathrm{C,opt}}$ and τ accentuates as τ increases, especially at higher values of the price ratio number P. A complementary aspect of these calculations is shown in Fig. 7: the refrigeration capacity number increases monotonically as τ_{C} increases while P is fixed, that is, as η_{II} describes the maxima revealed by Fig. 5. This means that the qualitative outlook of Fig. 5 remains unchanged if the abscissa parameter τ_{C} is replaced by Q^*.

The maximum second-law-efficiency curves pinpointed in this manner have been projected on the η_{II}–τ plane of Fig. 8, one curve for each P value. The ultimate conclusion of this analysis, then, is that in a fixed technological environment (constant P) the highest η_{II} values that can be attained decrease monotonically as τ increases. This conclusion matches in spirit the conclusion drawn already based on the simpler model (Fig. 2), however, at low temperatures (high τs) the slope of the $\eta_{\mathrm{II,max}}(\tau)$ curves (dashed lines of Fig. 8) is higher than the slope of the $\eta_{\mathrm{II}}(\tau)$ curves of Fig. 2. The apparent slope of the region covered in Fig. 2 by the empirical η_{II} data falls right between the two theoretical slopes. This can be seen easily by comparing Figs. 2 and 8.

Another interesting feature of each of the constant-P curves of Fig. 8 is that they drop off sharply as τ increases above a certain order of magnitude. This feature is a warning that unless technological innovations are adopted in order to decrease P, a given refrigeration plant technology (fixed P) fails at some point in the quest to reach absolute zero ($\tau \to \infty$). Indeed, a study of the history of large-scale low-temperature refrigeration techniques shows that each new step up in τ was preceded by the adoption of one or more new twists in the 'method' of refrigeration [12]. The current industrial example of a technological revolution of this kind is the proliferation of refrigeration plants the low temperature ends of which are occupied by a magnetic refrigeration (adiabatic demagnetization) stage [13]. This new generation of industrial refrigeration plants reaches into the T_{L} range 0.1–4.2 K, which on the abscissa of Fig. 8 corresponds to the τ range 71–3000.

Finally, despite the almost 100 years needed by our civilization to advance from left to right along the empirical horizontal bars of Fig. 8, the region covered by the empirical η_{II} data corresponds to a surprisingly narrow range of P values. One order-of-magnitude conclusion to retain is that the refrigeration and liquefaction plants that have been constructed are characterized by

$$P = \text{constant in the range } 0.02\text{–}0.05. \quad (33)$$

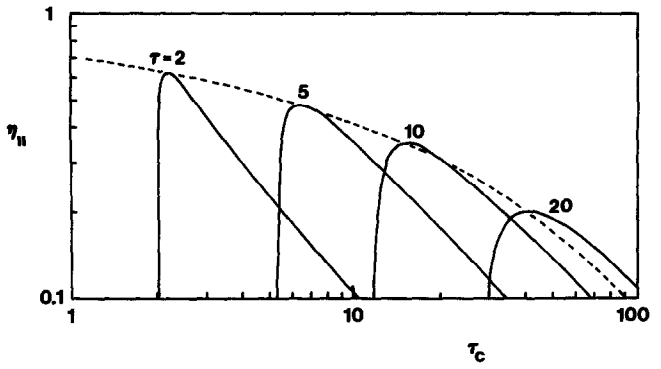

FIG. 5. The maximum second law efficiency attainable by a plant the refrigeration capacity of which has been maximized twice ($P = 0.03$).

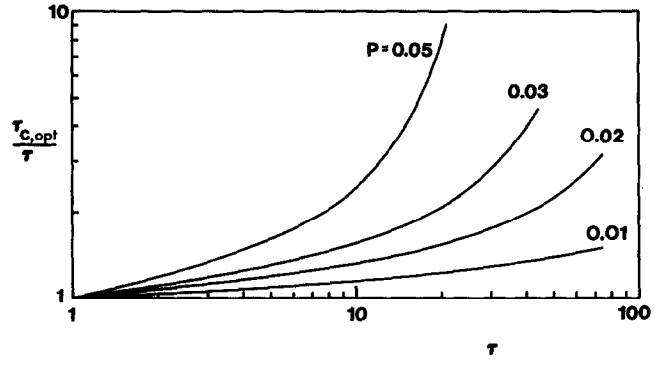

FIG. 6. The optimum Carnot temperature ratio corresponding to the η_{II} maxima illustrated in Fig. 5.

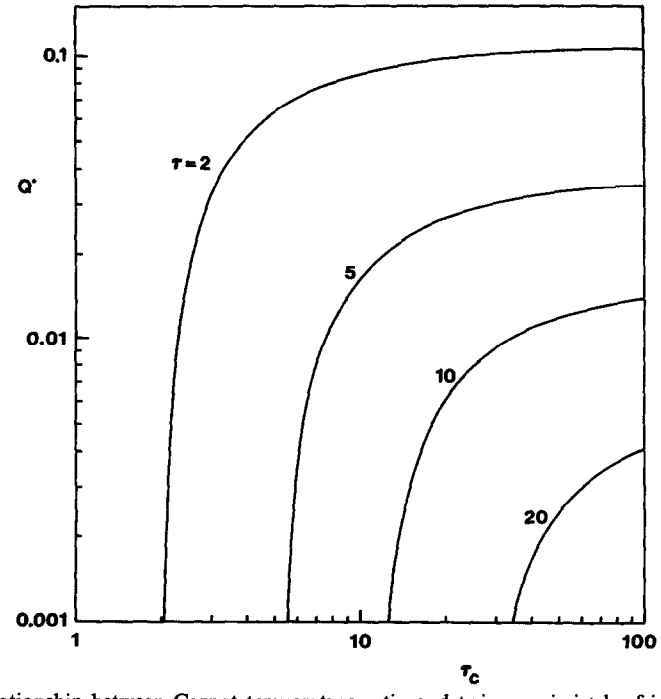

FIG. 7. The relationship between Carnot temperature ratio and twice-maximized refrigeration capacity when $P = 0.03$.

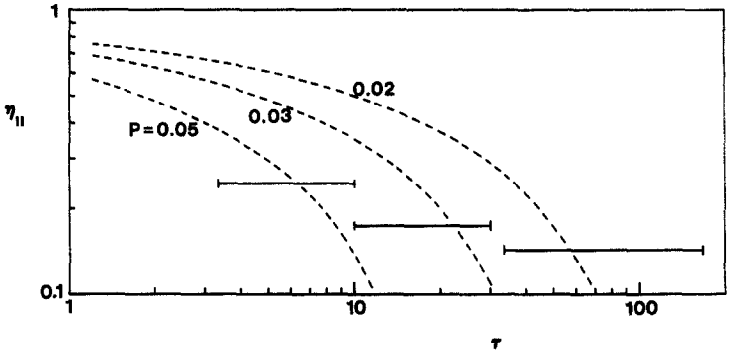

FIG. 8. Empirical data (horizontal bars) and the theoretical maximum-η_{II} curves predicted based on the second model.

The P constant appears to have migrated slightly toward lower values, as refrigeration technology reached toward lower temperatures. This means that in newer machines and in machines that operate at lower temperatures the unit price of the internal resistance has decreased relative to the unit price of the external conductance.

CONCLUSION

Looking back at the ground covered in this study, we see that two relatively simple theoretical arguments can be offered in order to refute the traditional reading of Fig. 1. It is quite possible that other, equally simple, arguments can come even closer to anticipating the downward slope of the empirical $\eta_{II}(\tau)$ data. This and the collection of more accurate η_{II} data for developing an empirical correlation in place of the three horizontal bars of Fig. 2 are items worthy of further study.

On a more fundamental plane, this analysis stresses the value of the 'simple model' in an era when more and more people are taught that 'complicated' systems should be analyzed automatically by computer. In the present study, two very simple models showed that the trend of the thermodynamic imperfection of the refrigeration plants that have been built in the modern era is explained largely by the heat transfer irreversibilities that have been retained in these models.

Acknowledgement—The support received from the National Science Foundation through Grant No. CBT-8711369 is gratefully acknowledged.

REFERENCES

1. A. Bejan, Theory of heat transfer-irreversible power plants, *Int. J. Heat Mass Transfer* **31**, 1211–1219 (1988).
2. T. R. Strobridge and D. B. Chelton, Size and power requirements of 4.2 K refrigerators, *Adv. Cryogen. Engng* **12**, 576–584 (1967).
3. T. R. Strobridge, Refrigeration for superconducting and cryogenic systems, *IEEE Trans. Nucl. Sci.* **NS-16**(3), Part 1, 1104–1108 (June 1969).
4. T. R. Strobridge, Cryogenic refrigerators—an updated survey, National Bureau of Standards Technical Note 655, Washington, DC (June 1974).
5. G. M. Reistad, Availability: concepts and applications, Doctoral dissertation, University of Wisconsin–Madison, University Microfilms International, Ann Arbor, Michigan (1970).
6. M. J. Moran, *Availability Analysis: a Guide to Efficient Energy Use*, Chap. 4. Prentice-Hall, Englewood Cliffs, New Jersey (1982).
7. R. V. Boyle and J. C. Riple, Turbines in the sky; the power behind Star Wars, *Mech. Engng* **109**, 38–45 (1987).
8. A. Bejan, A general variational principle for thermal insulation system design, *Int. J. Heat Mass Transfer* **22**, 219–228 (1979).
9. S. C. Collins and R. L. Cannaday, *Expansion Machines for Low Temperature Processes*. Oxford University Press, Oxford (1958).
10. J. A. Paivanas, A. W. Francis and D. I.-J. Wang, Insulation construction, U.S. Patent No. 3,133,422, 19 May (1964).
11. J. A. Paivanas, O. P. Roberts and D. I.-J. Wang, Multishielding—an advanced superinsulation technique, *Adv. Cryogen. Engng* **10**, 197–207 (1965).
12. A. Bejan, *Advanced Engineering Thermodynamics*, Chap. 10. Wiley, New York (1988).
13. J. A. Barclay, Magnetic refrigeration: a review of a developing technology, Paper CA-1, Cryogenic Engineering Conference, 14–18 June (1987).

THEORIE DE L'IRREVERSIBILITE PAR TRANSFERT DE CHALEUR POUR DES UNITES DE REFRIGERATION

Résumé—Cette étude pose la question du degré d'imperfection thermodynamique (efficacité η_{II} selon la seconde loi), de température de la réfrigération T_L. On montre d'abord que les valeurs empiriques η_{II} diminuent lorsque T_L augmente. Deux arguments théoriques sont offerts pour expliquer cela. Le premier d'entre eux est basé sur un modèle pour lequel l'irréversibilité est seulement due au transfert de chaleur "interne" qui passe directement à travers la machine vers T_L. Le second argument est basé sur un modèle plus fin dans lequel l'irréversibilité du système de réfrigération est due à trois phénomènes de transfert de chaleur; le transfert de chaleur interne (comme pour le premier modèle), la différence de température externe entre j'unité de réfrigération et l'ambiance, et la différence de température externe entre la charge de réfrigération et l'extrémité chaude de l'unité de réfrigération. On montre qu'il existe ds voies optimales dans des parties distinctes de l'unité, si l'objectif est d'optimiser la capacité de réfrigération. Ces arguments théoriques conduisent ensemble à conclure que généralement η_{II} décroît lorsque T_L augmente.

THEORIE DER WÄRMEÜBERTRAGUNG—IRREVERSIBLE KÄLTEANLAGEN

Zusammenfassung—In dieser Untersuchung wird die Vorstellung hinterfragt, daß der Grad der thermodynamischen Unzulänglichkeit (Wirkungsgrad nach dem Zweiten Hauptsatz η_{II}) bestehender Kälte- und Verflüssigungsanlagen nicht von der Kühllasttemperatur T_L abhängt. Es wird zunächst gezeigt, daß die empirisch ermittelten Werte für η_{II}, wenn sie korrekt dargestellt werden, mit sinkendem T_L abnehmen. Zwei theoretische Erklärungen für diesen Trend werden angeboten. Die erste basiert auf einem Kälteanlagenmodell, dessen Entropieerzeugung einzig auf dem "internen" Wärmetransport direkt durch die Anlage beruht, der bei T_L erfolgt. Die zweite Erklärung basiert auf einem verbesserten Modell, in dem die Entropie durch drei verschiedene Wärmeübertragungsvorgänge erzeugt wird: den internen Wärmetransport (auch im ersten Modell enthalten), die externe Temperaturdifferenz zwischen Kälteanlage und Umgebung und die externe Temperaturdifferenz zwischen Kühllast und kalter Seite der Kälteanlage. Es wird gezeigt, daß optimale Strategien für die Verteilung von Wärmeübertragungseinrichtungen an die unterschiedlichen Teile der Anlage bestehen, wenn das Ziel die Maximierung der Kühlleistung der Anlage ist. Beide theoretische Erklärungen führen zu der Schlußfolgerung, daß η_{II} generell mit sinkendem T_L abnimmt.

ТЕОРИЯ ТЕПЛОПЕРЕНОСА В ПРИЛОЖЕНИИ К ХОЛОДИЛЬНЫМ УСТАНОВКАМ С НЕОБРАТИМЫМ ЦИКЛОМ

Аннотация—Оспаривается утверждение, что степень термодинамической неидеальности (коэффициент эффективности по второму закону, η_{II}) холодильных и ожижительных установок не зависит от температуры нагрузки T_L. Показано, что при правильном графическом представлении эмпирические значения η_{II} падают с уменьшением T_L. Предложены два теоретических соображения для объяснения этой тенденции. Первое основано на модели холодильной установки, необратимость работы которой обусловлена исключительно "внутренним" теплопереносом через установку вплоть до температуры T_L. Второе базируется на более сложной модели, в которой необратимость холодильной установки обязана трем явлениям теплопереноса: внутреннему теплопереносу (учитываемому также первой моделью), разности температур установки и окружающей среды и разности температур между тепловой нагрузкой холодильной установки и холодной частью установки. Показано, что за счет оптимального размещения теплообменного оборудования в холодильных установках можно увеличить их охлаждающую способность. В обоих вариантах значения η_{II} как правило падают с уменьшением T_L.